



Published in final edited form as:

*J Thorac Cardiovasc Surg.* 2015 July ; 150(1): 28–35.e1. doi:10.1016/j.jtcvs.2015.05.014.

## Intraoperative Molecular Imaging Can Identify Lung Adenocarcinomas during Pulmonary Resection

Olugbenga T. Okusanya, MD<sup>1</sup>, Elizabeth M. DeJesus, BA<sup>1</sup>, Jack X. Jiang, BS<sup>1</sup>, Ryan P. Judy, BA<sup>1</sup>, Ollin G. Venegas, BA<sup>1</sup>, Charuhas G. Deshpande, MD<sup>2</sup>, Daniel F. Heitjan, PhD<sup>3</sup>, Shuming Nie, PhD<sup>4</sup>, Philip S. Low, PhD<sup>5</sup>, and Sunil Singhal, MD<sup>1,\*</sup>

<sup>1</sup>Department of Surgery, University of Pennsylvania Perelman School of Medicine

<sup>2</sup>Department of Pathology, University of Pennsylvania Perelman School of Medicine

<sup>3</sup>Department of Biostatistics & Epidemiology, University of Pennsylvania

<sup>4</sup>Departments of Biomedical Engineering and Chemistry, Emory University

<sup>5</sup>Department of Chemistry, Purdue University

### Abstract

**Background**—Over 80,000 people undergo resection of a pulmonary tumor each year, and the only method to determine if the tumor is malignant is histological analysis. We propose that a targeted molecular contrast agent could bind lung adenocarcinomas and then identify these tumors by real-time optical imaging at the time of surgery.

**Methods**—Fifty patients with a biopsy-proven lung adenocarcinoma were enrolled. Prior to surgery, patients were systemically administered 0.1 mg/kg of a fluorescent folate receptor alpha (FR $\alpha$ )-targeted molecular contrast agent by intravenous infusion. During surgery, tumors were imaged *in situ* and *ex vivo* after dissecting the lung parenchyma to directly expose the tumor to the imaging system.

**Results**—Tumors ranged from 0.3—7.5 cm (mean 2.6cm), and 46/50 (92%) lung adenocarcinomas were fluorescent. There was no false uptake, and in 2 cases, intraoperative imaging discovered tumor metastases (3mm and 6mm) that were not recognized preoperatively. Four adenocarcinomas were not fluorescent, and immunohistochemistry showed these adenocarcinomas did not express FR $\alpha$ . Tumor fluorescence was independent of nodule size, <sup>18</sup>FDG uptake, histology, and tumor differentiation. Molecular imaging could only identify 7 out of the 50 adenocarcinomas *in situ* in the patient without bisection. The most important predictor of molecular imaging to locate the tumor *in situ* was the distance of the nodule from the pleural surface.

---

Corresponding Author: Sunil Singhal, University of Pennsylvania School of Medicine, 3400 Spruce Street, Philadelphia, PA 19104, sunil.singhal@uphs.upenn.edu.

**Disclosures:** SN is a consultant for SpectroPath, Inc., a startup company to develop advanced instrumentation and nanoparticle contrast agents. PSL is a consultant and stake holder in OnTarget Laboratories LLC.

**Publisher's Disclaimer:** This is a PDF file of an unedited manuscript that has been accepted for publication. As a service to our customers we are providing this early version of the manuscript. The manuscript will undergo copyediting, typesetting, and review of the resulting proof before it is published in its final citable form. Please note that during the production process errors may be discovered which could affect the content, and all legal disclaimers that apply to the journal pertain.

**Conclusions**—Intraoperative molecular imaging with a targeted contrast agent can identify lung adenocarcinomas, and this technology is currently useful in patients with subpleural tumors irrespective of size. With further refinements, this tool may prove useful in locating adenocarcinomas deeper in the lung parenchyma, lymph nodes and at pleural and resection margins.

---

## Introduction

Each year, hundreds of thousands of people are discovered to have a pulmonary nodule or mass on radiological exams in the US, and 80,000 patients ultimately go to surgery for removal.<sup>1-3</sup> Currently, the only method to determine if the nodule or mass is malignant is histological examination. As an alternative, our group and others have proposed using targeted molecular optical imaging probes to specifically bind and identify malignant cells.<sup>4-10</sup>

Molecular imaging is a technique by which contrast agents are used to identify a target on tumor cells. For example, position emission tomography (PET) scanning is one type of molecular imaging. It is used to evaluate lung nodules using 2-deoxy-2-(<sup>18</sup>F)fluoro-D-glucose (<sup>18</sup>FDG), the only FDA approved molecular contrast agent. <sup>18</sup>FDG binds the GLUT1 receptor on tumor cells. However, despite the common use of <sup>18</sup>FDG-PET scanning, it is not selective for malignant cells.

Thus, a strategy using targeted optical molecular contrast agents specific to cancer cells is appealing. Van Dam and colleagues recently published a report using molecular imaging during surgery to identify ovarian cancers during abdominal exploration.<sup>11</sup> Their study used a visible wavelength molecular tracer to intraoperatively locate epithelial ovarian tumors. However, for lung cancer, no human study has demonstrated the successful use of targeted molecular imaging to identify pulmonary adenocarcinomas.

Lung adenocarcinomas have significantly greater expression of folate receptor alpha (FR $\alpha$ ) compared to normal lung epithelium.<sup>12, 13</sup> In preliminary studies, we first studied the specificity of a targeted fluorescent molecular imaging contrast agent, folate-fluorescein-isothiocyanate (folate-FITC), to FR $\alpha$  on human lung adenocarcinoma cell lines. Molecular imaging could identify as few as 10<sup>4</sup> cancer cells in ideal conditions. Follow-up studies in murine studies demonstrated an 8 to 10 fold increased fluorescent signal in orthotopic lung tumors compared to normal lung parenchyma, and molecular imaging could locate nodules as small as 0.5 mm. Finally, we performed *in vitro* analyses of more than 100 human tumors confirming that FR $\alpha$  is highly expressed (10<sup>3</sup>-10<sup>4</sup> receptors/cell) on lung adenocarcinomas, and folate-FITC has 80% to 90% specificity for pulmonary adenocarcinomas.<sup>13</sup> Based on these data, we postulated FR $\alpha$  could be an appealing molecular target for optical imaging to identify lung adenocarcinomas during surgery in humans.

The goal of this study was to determine if an optical targeted molecular contrast agent to FR $\alpha$  could bind lung adenocarcinomas and if these tumors could then be identified by real-time optical imaging either *in situ* or *ex vivo* at the time of surgery. As a proof-of-principle in order to accomplish this goal, 50 patients with known lung adenocarcinomas were given

systemic doses of a targeted folate-FITC conjugate, and then their tumors were imaged in the operating room.

## Methods

### Clinical Study Design

This clinical study was approved by the University of Pennsylvania and Philadelphia Veterans Affairs Medical Center Institutional Review Boards and informed consent was obtained from all patients. Patients with a biopsy-proven lung adenocarcinoma were eligible for this study. All patients underwent preoperative staging with a chest computed tomography (CT) scan with 0.1 cm slice thickness and an <sup>18</sup>F-FDG-PET scan, which showed with no evidence of extrathoracic metastatic disease. No patients received preoperative chemotherapy or radiation therapy. All patients were instructed to stop folate-containing vitamins one week prior to surgery. All preoperative tissue biopsies were interpreted at our institution by a pathologist specializing in thoracic diseases. Patients who were scheduled for a video-assisted thoracoscopic or robot-assisted pulmonary resection were excluded due to the limitations of our imaging equipment.

Four hours prior to surgery, patients were administered 0.1mg/kg of the folate-FITC conjugate (On Target Laboratories, Inc., W. Lafayette, IN) intravenously. At thoracotomy, the primary lesion was located using traditional methods using visual inspection and manual palpation. The gantry-mounted intraoperative fluorescent imaging system, sterilely draped, was positioned above the chest using a custom designed positioning device (BioMediCon, Moorestown, NJ). The operating room lights were then switched off, and the cancer was then imaged and photo-documented by fluorescence and white light *in situ*. Imaging was performed on the deflated lung in order to facilitate exposure of the imaging system to as much of the surface of the lung as possible.

Once removed, the lung parenchyma overlying the tumor was carefully bisected. Care was taken not to disrupt pleural and hilar margins for the pathologist, and to provide close-up molecular imaging of the tumor. Frozen section biopsies were performed when indicated. All specimens were sent for permanent histopathology. Final specimens were reviewed by a specialized lung pathologist.

### Optical molecular fluorescence imaging

Intraoperative imaging was performed using the Artemis Fluorescence Imaging system (Quest Medical Imaging, the Netherlands), FloCam (BioVision, Exeter, PA), or a prototype system developed in our laboratory (see Supplemental Figure 1 and reference #13).<sup>14</sup> Positive and negative controls were used prior to each operation to confirm the camera was functioning. In order to quantitate the tissue fluorescence, region-of-interest software and HeatMap plugin within ImageJ (<http://rsb.info.nih.gov/ij/>; public domain free software developed by National Institutes of Health) were used. A background reading was taken from adjacent normal lung tissue in order to generate a tumor-to-background ratio (TBR).

## Immunohistochemistry and fluorescence microscopy

Formalin-fixed, paraffin-embedded samples were stained for FR $\alpha$  with mAb343 (1.8 mg/mL) by standard protocols previously described.<sup>14</sup> Staining was graded from zero (no positive staining) to 3+ (>80% of cells staining), and then averaged for 3 high powered fields from the same tumor specimen. An average score of 0 was defined as no expression, 1 was defined as weak expression while an average score of 2 or 3 was defined as strong expression. To detect FITC, the monoclonal antibody Mab10257 (Abcam®) was used after cell membrane permeabilization with methanol.

Lastly, a punch biopsy of the tumor was taken in the operating room after the tumor was excised. This biopsy was frozen, sectioned and imaged using fluorescence microscopy. Fluorescence microscopy was performed using an Olympus IX51 fluorescent microscope equipped with a FITC-specific filter set (Chroma® 49012). Data from fluorescence microscopy were compared to the subjective and quantitative measurements of fluorescence.

## Flow Cytometry

A portion of the punch biopsy from fresh lung tumors were also processed for flow cytometry within 30 minutes of removal as previously described.<sup>15</sup> Tumor fragments were sliced into small pieces and enzymatically digested with a cocktail composed of multiple collagenases and elastase (Worthington) for one hour at 37 C° with continuous shaking. After RBC lysis, cell viability was determined by trypan blue exclusion. If the viability of cells was less than 80%, dead cells were eliminated using a “dead cell removal kit” (Miltenyi Biotec Inc., Germany). Flow cytometric analysis was performed according to standard protocols.<sup>16</sup> Matched isotype antibodies were used as controls. Data was acquired using the FACSCalibur™ or LSRFortessa™ flow cytometers (both from BD Biosciences) and was analyzed using FlowJo software (Tree Star, Ashland, OR, USA).

## Data Analysis

The significance of differences in median values (size, tumor-to-background ratio (TBR), depth on CT scan and standard uptake value (SUV)) of non-fluorescing vs. fluorescing tumors were assessed by the Mann-Whitney test. Differences in paired samples were tested using the Wilcoxon signed-rank test. Correlation of continuous outcomes was assessed by the Pearson correlation coefficient. All analyses were performed in SAS Version 9.3 (SAS Institute, Inc.; Cary, NC).

## Results

### FR $\alpha$ -targeted molecular imaging can identify pulmonary adenocarcinomas

Between January 2013 and March 2014, 50 patients between the ages of 25 and 85 (mean 67) with biopsy-proven lung adenocarcinoma were enrolled in this study. Radiographically, the mean tumor size in the study was  $2.6 \pm 1.9$  cm (range 1.0 to 7.5), and the mean standard uptake value (SUV) on <sup>18</sup>FDG-PET was  $5.1 \pm 3.7$  (range not detected to 19) (Table 1).

In 7 out of the 50 (14%) cases, the tumor was fluorescent *in situ* before excising the tumor. In these cases, the mean tumor-to-background ratio (TBR) of the nodule was  $3.6 \pm 1.2$

(range 2.0-6.1). These 7 *in situ* fluorescent tumors ranged in size from 1.1 to 8.0 cm (mean 3.1 cm). On preoperative CT, all 7 of these tumors were subpleural and within 1.2 cm of the surface of the lung.

Following excision and direct exposure of the tumor, 39 of the remaining 43 tumors were fluorescent (Fig. 1). The mean TBR of the tumors was  $4.2 \pm 2.7$  (range 2.0–14.7). The fluorescence appeared uniform across the entire surface of the tumor, and the signal was sharply demarcated from the surrounding lung parenchyma irrespective of peritumoral atelectasis or inflammation. In total, *in situ* optical imaging required a mean of 8 minutes (range 5-15 minutes) to perform.

Four tumors did not exhibit fluorescence *in situ* or after bisection. The mean *ex vivo* TBR of these 4 non-fluorescent tumors was 0.96 (range 0.9 – 1.1). The average size of these lesions was 2.6 cm (range 1.3 to 3.5 cm). Of the 46 lung adenocarcinomas demonstrating fluorescence either *in situ* or *ex vivo*, we found no correlation between the size of the nodule and the *in situ* TBR or *ex vivo* TBR ( $p>0.05$ ). There was no correlation between SUV value and TBR *in situ* or *ex vivo* ( $p>0.05$ ). Tumors at either end of the size range displayed bright fluorescence. The mean size of these 46 tumors ranged from 1.0 to 7.5 cm (mean 2.6 cm).

### Validation by Pathology, Immunohistochemistry and Fluorescence Microscopy

On final pathology, all fifty tumors were ultimately confirmed to be adenocarcinomas. There were 18 poorly or un-differentiated tumors, 23 moderately differentiated tumors and 9 well differentiated tumors with 24 acinar, 9 papillary, 3 solid, 7 lepidic and 7 mixed histologic subtypes. 47 of the tumors were invasive while 3 were adenocarcinoma *in situ* (non-invasive) or minimally invasive adenocarcinoma (<5 mm focus of invasion) (Table 1). The four tumors that were not fluorescent were all invasive adenocarcinomas: 2 poorly differentiated, 1 moderately differentiated and 1 well differentiated. They were 2 acinar tumors, 1 papillary and 1 mixed histology subtype tumors. For fluorescent and non-fluorescent tumors, there was no correlation between the FR $\alpha$  expression or TBR versus subtype or degree of tumor differentiation ( $p>0.05$ ).

All 46 tumors demonstrating fluorescence in the operating room also showed microscopic fluorescence on the tumor cells which co-registered with the H&E staining. These tumors were also stained for FR $\alpha$ , and all 46 tumors expressed this receptor. To further confirm that the fluorescence was detected from the contrast agent attached to the tumor cell and not autofluorescence, the slides were counter-stained with an anti-FITC antibody. In all cases, strong anti-FITC staining was found in the samples. (Fig. 2) The four lesions that were not fluorescent were also stained for FR $\alpha$ , and none expressed FR $\alpha$  or anti-FITC. This data shows the FR $\alpha$ -targeted molecular contrast agent has high sensitivity (100%) for localizing to FR $\alpha$ <sup>+</sup> lung adenocarcinomas.

### Limitation of *in situ* fluorescent molecular imaging

Intraoperatively, only 7 of the lung adenocarcinomas demonstrated identifiable fluorescence *in situ* even though 92% demonstrated obvious fluorescence once their surface was exposed (Fig. 3). To explain the difficulty in obtaining fluorescent images *in situ*, the difference in the TBR from the tumor in and out of the patient was analyzed.

First, the TBR from the tumor *in situ* and *ex vivo* before bisecting the specimen were compared. Despite the superior control of external factors such as proximity of camera and reduction of ambient light, the mean *in situ* and *ex vivo* TBR was 1.6 versus 1.7 ( $p=0.27$ ), respectively (Fig. 4a). Thus, this suggests that physically removing the specimen from the chest made no difference in the TBR.

Next, the TBR from the tumor *ex vivo* before and after directly exposing the tumor to the imaging system were compared. Grossly, 45 of the 50 tumors had an improved TBR after dissecting the specimen. The mean nodule TBR before and after tumor exposure (1.7 versus 4.2) was significantly greater ( $p=0.001$ ) (Fig. 4b).

Given these findings, it was speculated that the TBR was dependent on the depth of the tumor from the pleural surface. The nodule depth on CT scan was compared to the nodule TBR *in situ*. The nodule depth was defined as the distance from the pleural surface to the outer rim of the nodule in the inflated lung. These measurements were based on the preoperative CT scan, using the closest distance on serial images from coronal, sagittal and axial windows. Tumors into two groups: tumors abutting the pleural surface and those tumors not at the pleural surface. The mean *in situ* TBR of the nodules at the pleura ( $<1.2$  cm) was statistically greater than the TBR of the nodules below the pleural surface ( $p=0.044$ ) (Fig. 4c).

In summary, the depth of the tumor in the lung appears to be the most significant limiting factor in successful tumor detection by intraoperative molecular imaging with folate-FITC.

## Clinical Findings

All patients received 0.1 mg/kg of the FR $\alpha$ -targeted fluorescent molecular probe (folate-FITC) four hours prior to surgery without complications. There was no toxicity associated with the injection of the folate-FITC, though one patient developed mild hives which resolved with a single dose of intravenous diphenhydramine. Another patient had some irritation at the injection site which resolved by slowing the infusion. All patients were discharged from the hospital alive within 30 days of surgery.

Two cases deserve special note. The first was a 50 year-old male with a 2.1 cm primary lung adenocarcinoma in the right upper pulmonary lobe. CT and PET images were reviewed by a radiologist and suggested the presence of no additional nodules. The patient underwent a right thoracotomy and right upper lobectomy. On the back table, molecular imaging of the excised lobe then identified an incidental second pulmonary nodule that was fluorescent (Fig. 5). Final pathology demonstrated a 0.6 cm synchronous pulmonary adenocarcinoma, thus the patient was re-staged from Stage IA (T1N0) to Stage IIB (T3N0).

Second, a 60 year-old male with a 2.6 cm left lower lobe nodule was scheduled for a routine lobectomy. At the time of surgery, before *in vivo* imaging, the surgeon did not appreciate any evidence of metastatic disease. However, during the molecular imaging, a small pleural implant on the parietal surface near the costophrenic sulcus was fluorescent. Thus, it was removed and sent for frozen section analysis. This lesion was positive for a  $<3$  mm



metastatic adenocarcinoma. Due to the presence of Stage IV disease, the primary lesion was removed by wedge excision and the chest was closed with no further resection.

## Discussion

This pilot clinical trial shows that optical fluorescent molecular imaging can be used to visually identify adenocarcinomas of the lung. This modality is independent of tumor size, histologic subtype and differentiation, and SUV value on PET scanning. These data simultaneously expose an important limitation related to tumor depth from the pleural surface, although this issue is likely surmountable. With refinements, molecular imaging with targeted optical probes may have valuable application as an intraoperative diagnostic tool to identify positive margins, lymph nodes with metastatic cancer cells and synchronous pulmonary lesions.

Our molecular contrast agent, folate-fluorescein isothiocyanate (folate-FITC), is a conjugate between folate and fluorescein isothiocyanate. This conjugate forms a negatively charged fluorescent molecule that binds weakly and non-specifically to serum proteins at a level of ~75%. FITC is a synthetic organic compound that is excited in the 465-490 nm wavelength and emits light in the 520-530 nm range (visible spectrum). In addition, in normal lung pneumocytes, FR $\alpha$  is expressed on the apical (luminal) side of polarized epithelial cells; thus it has no access to systemically administered folate.<sup>17-19</sup> For lung adenocarcinomas, our laboratory has found that it is a reasonable molecular target for imaging. Therapeutically, there are limitations to FR $\alpha$  to delivery toxic agents because it is also present on the kidney and choroid plexus. Of note, these results may give impetus to the search for similar molecules to target other tumor types (non-adenocarcinoma) of the lung.

We believe the most important finding in this study was the ability to systemically inject our contrast agent into patients prior to surgery, and have 92% of the lung adenocarcinomas fluoresce in the operating room. Other contrast agents for molecular imaging of lung adenocarcinomas have significant limitations. <sup>18</sup>F-FDG-PET imaging is based on metabolic activity and is non-specific. Another strategy using indocyanine green as the contrast agent takes advantage of the enhanced permeability and retention effect, whereby colloidal or aggregated contrast agents tend to accumulate in tumors due to “leaky” capillaries.<sup>5, 7</sup> Again, this approach is also non-specific.<sup>4, 6</sup> In this work, targeting the fluorescent probe to FR $\alpha$  appears to be highly specific. We did not observe non-specific binding in peritumoral tissues, atelectasis or inflammation, which has been a source of false positive uptake with other contrast agents. Furthermore, our contrast agent accumulates in sufficient concentrations *in vivo* that it can be detected by standard molecular imaging devices without spectral unmixing or significant enhancement.

There are three other key advantages to this imaging strategy. First, we discovered that this imaging technique can locate tumors with a wide range of sizes (3 mm to 7.5 cm), pathological subtypes and metabolic activity. The tumor-to-background ratio was not markedly different in small, poorly differentiated or metabolically inactive tumors. This finding demonstrates that intraoperative molecular imaging may be potentially broadly applicable to all FR $\alpha$ <sup>+</sup> lung tumors. Second, this technology is safe. The use of a visible

wavelength fluorophore avoids ionizing radiation and confers no risk to the patient, surgeon or operating room personnel. In our experience, only one patient had a mild allergic reaction to the contrast agent that was easily managed with diphenhydramine. Third, optical imaging is easily understood by surgeons with no need for special training to interpret or process the data.

The biggest drawback of our molecular contrast agent was the lack of depth of penetration into the lung parenchyma. There is some degree of attenuation of the fluorescent signal as it passes through the tissues. Practically, this would limit the current technology to subpleural tumors which are likely palpable or may be visualized by the surgeon. This study demonstrates that the fluorescent moiety (FITC) in the targeted probe we used is not an ideal contrast agent for tumors deep in the lung parenchyma. Two potential solutions exist to overcome this problem. First, we are exploring the possibility of using spectroscopic tools to analyze the scatter from the FITC; this would allow a deeper depth of penetration, as much as several centimeters into the solid organ. A second approach would be to re-design the tracer for near-infrared capabilities (i.e. emission > 700 nm). Due to the greater tissue penetration and reduced autofluorescence of near infrared light, such a tracer would allow detection of nodules buried deeper beneath the overlying healthy parenchyma.

Although this study was a proof-of-principle pilot study, it had two interesting findings which provide anecdotal support for the value of molecular imaging during pulmonary resection. First, this method identified a second pulmonary nodule that was not identified on the preoperative CAT scan. Second, intraoperative imaging discovered a subpleural metastasis that would have been difficult to discriminate from the native tissues without contrast enhancement. This approach may allow surgeons to perform resections with confidence that the entire tumor burden has been eliminated. In the future, with improved devices and molecular contrast agents, this approach may reduce the local recurrence rate and improve intraoperative identification of metastatic cancer cells.

Finally, we point out that one of the major applications to this technology may be minimally invasive surgery. Unlike traditional open surgery, minimally-invasive surgery by video-assistance or robotics limits palpation of the lung and is the main disadvantage of these approaches. Thus, with improvement, this technology may be useful during minimally invasive surgery for inspecting and locating nodules. Miniaturization of imaging devices for visualizing fluorescent dyes is currently in development by many commercial vendors.

## Supplementary Material

Refer to Web version on PubMed Central for supplementary material.

## Acknowledgments

**Funding:** The project described was partially supported by Award Number I011CX001189 (SS, CD) from the Biomedical Laboratory Research & Development Service of the VA Office of Research and Development and by the CHEST Foundation One Breath Clinical Research Award (SS). We would like to thank Dr. Joel D. Cooper, Professor of Surgery at the University of Pennsylvania School of Medicine, for his invaluable input and guidance in this body of work.



## References

1. Siegel R, Naishadham D, Jemal A. Cancer statistics, 2013. *CA Cancer J Clin.* 2013; 63:11–30. [PubMed: 23335087]
2. 2013 United States Procedure Volumes Database. Thomas Reuters; United States: 2013.
3. Agency for Healthcare Research and Quality; 2011. National Inpatient Sample (NIS). <http://www.hcup-us.ahrq.gov/nisoverview.jsp>
4. Holt D, Okusanya O, Judy R, Venegas O, Jiang J, DeJesus E, et al. Intraoperative Near-Infrared Imaging Can Distinguish Cancer from Normal Tissue but Not Inflammation. *PLoS ONE.* 2014; 9:e103342. [PubMed: 25072388]
5. Madajewski B, Judy BF, Mouchli A, Kapoor V, Holt D, Wang MD, et al. Intraoperative near-infrared imaging of surgical wounds after tumor resections can detect residual disease. *Clin Cancer Res.* 2012; 18:5741–51. [PubMed: 22932668]
6. Okusanya OT, Holt D, Heitjan D, Deshpande C, Venegas O, Jiang J, et al. Intraoperative Near-Infrared Imaging Can Identify Pulmonary Nodules. *Ann Thorac Surg.* 2014
7. Singhal S, Nie S, Wang MD. Nanotechnology applications in surgical oncology. *Annu Rev Med.* 2010; 61:359–73. [PubMed: 20059343]
8. Savariar EN, Felsen CN, Nashi N, Jiang T, Ellies LG, Steinbach P, et al. Real-time in vivo molecular detection of primary tumors and metastases with ratiometric activatable cell-penetrating peptides. *Cancer Res.* 2013; 73:855–64. [PubMed: 23188503]
9. Frangioni JV. New technologies for human cancer imaging. *J Clin Oncol.* 2008; 26:4012–21. [PubMed: 18711192]
10. Okusanya OT, Deshpande C, Barbosa EM, Aggarwal C, Simone CB II, Jiang J, et al. Molecular imaging to identify tumor recurrence following chemoradiation in a hostile surgical environment. *Mol Imaging.* 2014; 13:1–6.
11. van Dam GM, Themelis G, Crane LM, Harlaar NJ, Pleijhuis RG, Kelder W, et al. Intraoperative tumor-specific fluorescence imaging in ovarian cancer by folate receptor-alpha targeting: first in-human results. *Nat Med.* 2011
12. Weitman SD, Lark RH, Coney LR, Fort DW, Frasca V, Zurawski VR Jr, et al. Distribution of the folate receptor GP38 in normal and malignant cell lines and tissues. *Cancer Res.* 1992; 52:3396–401. [PubMed: 1596899]
13. O'Shannessy DJ, Yu G, Smale R, Fu YS, Singhal S, Thiel RP, et al. Folate Receptor Alpha Expression in Lung Cancer: Diagnostic and Prognostic Significance. *Oncotarget.* 2012
14. Okusanya OT, Madajewski B, Segal E, Judy BF, Venegas OG, Judy RP, et al. Small Portable Interchangeable Imager of Fluorescence for Fluorescence Guided Surgery and Research. *Technol Cancer Res Treat.* 2013
15. Eruslanov EB, Bhojnagarwala PS, Quatromoni JG, Stephen TL, Ranganathan A, Deshpande C, et al. Tumor-associated neutrophils stimulate T cell responses in early-stage human lung cancer. *J Clin Invest.* 2014
16. Predina J, Eruslanov E, Judy B, Kapoor V, Cheng G, Wang LC, et al. Changes in the local tumor microenvironment in recurrent cancers may explain the failure of vaccines after surgery. *Proc Natl Acad Sci U S A.* 2013; 110:E415–24. [PubMed: 23271806]
17. Ross JF, Chaudhuri PK, Ratnam M. Differential regulation of folate receptor isoforms in normal and malignant tissues in vivo and in established cell lines. Physiologic and clinical implications. *Cancer.* 1994; 73:2432–43. [PubMed: 7513252]
18. Parker N, Turk MJ, Westrick E, Lewis JD, Low PS, Leamon CP. Folate receptor expression in carcinomas and normal tissues determined by a quantitative radioligand binding assay. *Anal Biochem.* 2005; 338:284–93. [PubMed: 15745749]
19. Mantovani LT, Miotti S, Menard S, Canevari S, Raspagliesi F, Bottini C, et al. Folate binding protein distribution in normal tissues and biological fluids from ovarian carcinoma patients as detected by the monoclonal antibodies MOv18 and MOv19. *Eur J Cancer.* 1994; 30A:363–9. [PubMed: 8204360]

**Central Message**

Intraoperative imaging using targeted molecular agents can cause lung adenocarcinomas to fluoresce during pulmonary surgery.

Author Manuscript

Author Manuscript

Author Manuscript

Author Manuscript

### Perspective

New molecular tools are emerging to identify lung adenocarcinomas during pulmonary resection. This technology will permit precise visualization of tumor margins, localization of small malignant ground glass opacities, and accurate selection of lymph nodes with metastatic cancer cells. With miniaturization of imaging devices, this method will be particularly useful in minimally-invasive surgery.

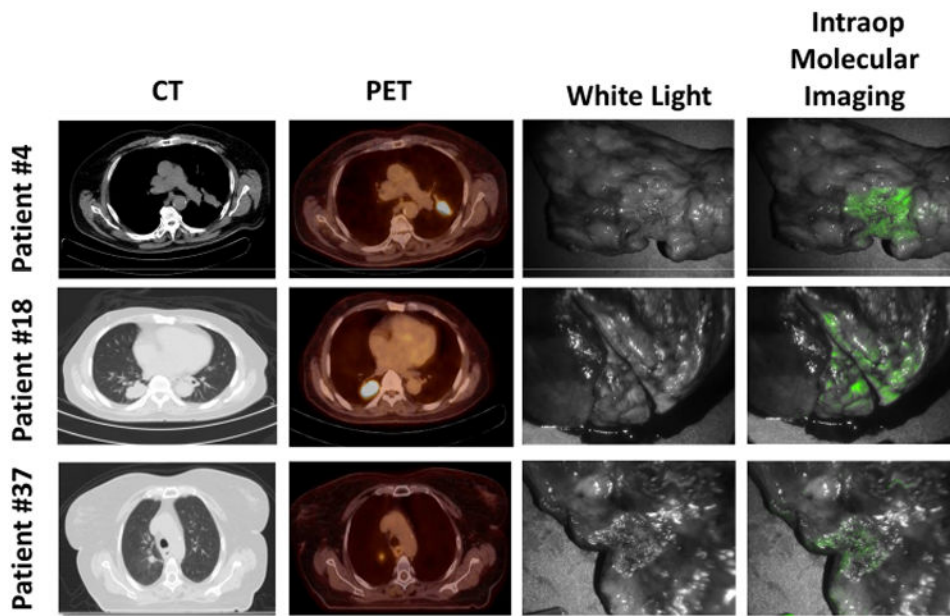


**Figure 1.** Lung adenocarcinomas can be detected using intraoperative molecular imaging. Three representative patients diagnosed with lung adenocarcinoma by preoperative CT, PET and optical molecular imaging.

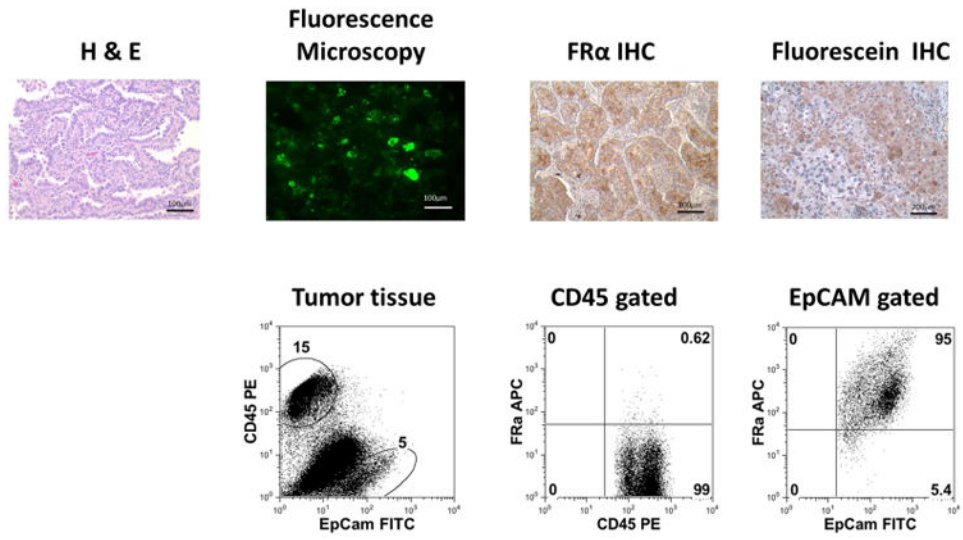


**Figure 2.** Tumor specimens were confirmed to be adenocarcinomas and to uptake folate-FITC by H&E, fluorescence microscopy, FR $\alpha$  IHC and FITC IHC stains and flow cytometry.

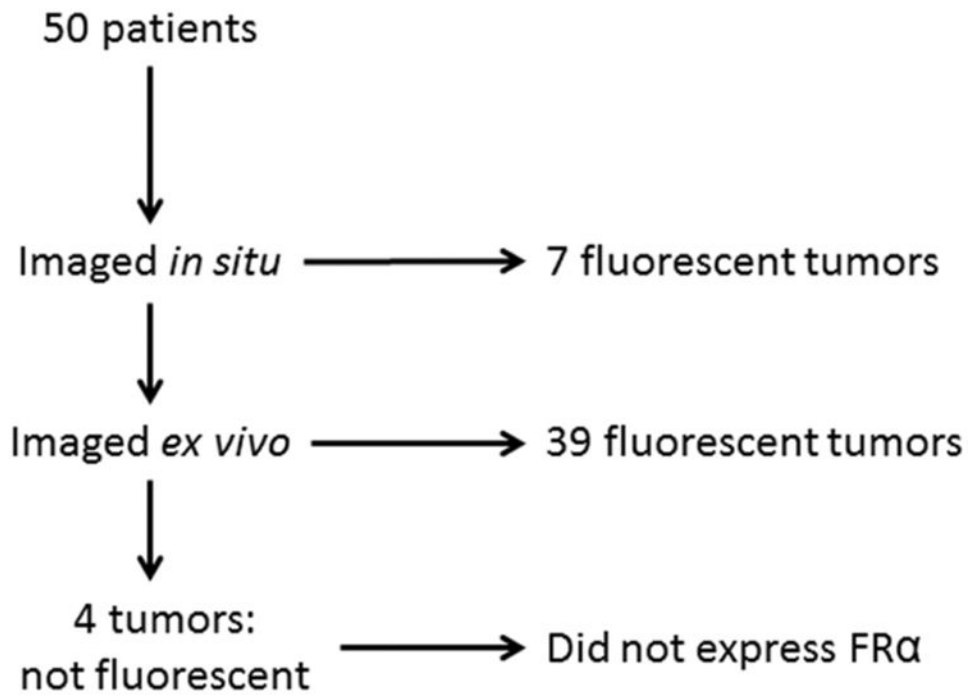


**Figure 3.** Summary of results of intraoperative imaging of 50 patients with pulmonary adenocarcinomas.



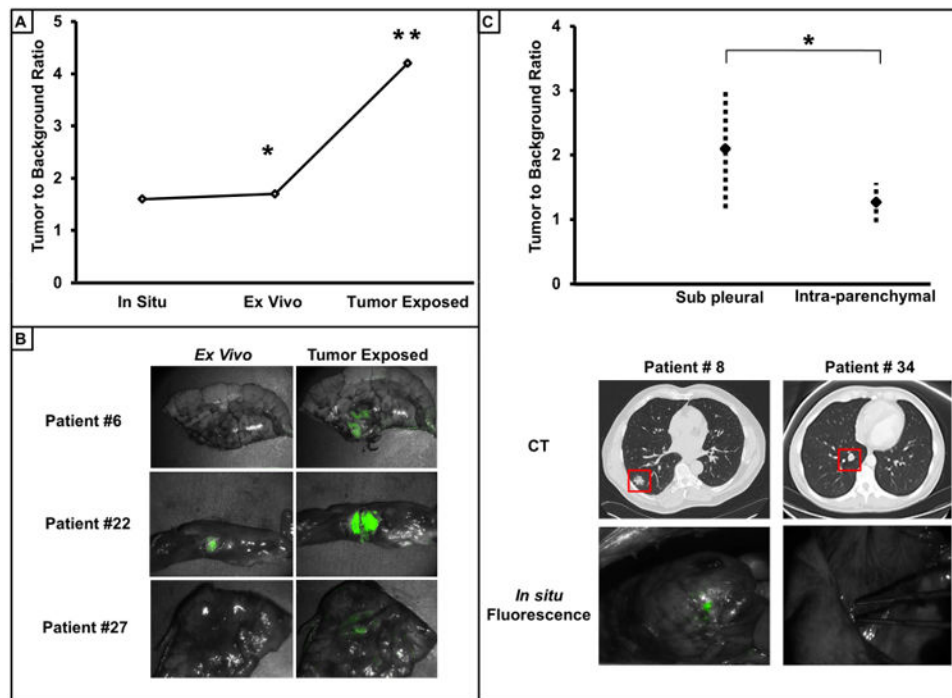


**Figure 4.**

Depth of penetration is a limitation of intraoperative molecular imaging. A) Qualitative representative comparisons of TBR of tumors in the *in situ*, *ex vivo* and tumor exposed setting. \* For all tumor sample there was no statistical difference ( $p=0.27$ ) between TBR in the *in situ* and *ex vivo* setting. \*\* TBR of tumors when exposed was significantly greater ( $p<0.001$ ) than in the *ex vivo* setting. B) Representative comparison of the difference in tumor TBR *ex vivo* before and after exposing the surface of the tumor. C.) TBR of pleural based tumors versus tumors deep in the lung parenchyma. Representative example of CT and *in situ* images demonstrate the qualitative difference.

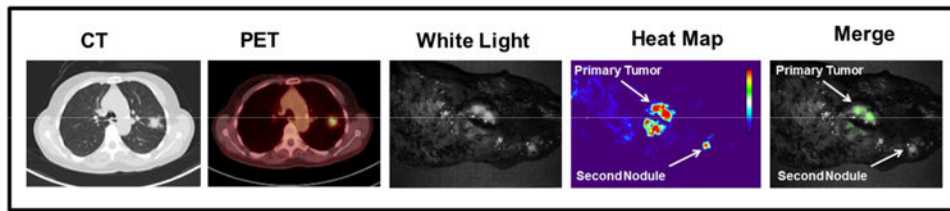
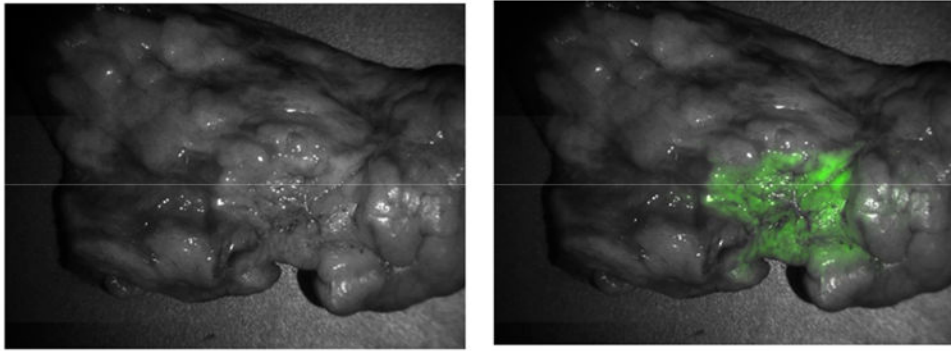


**Figure 5.** Clinical implications of intraoperative imaging. A 50 year-old with a 2 cm adenocarcinoma diagnosed by CT and PET scan showing no other sites of disease. Intraoperative molecular imaging was able to detect a synchronous nodule in the same pulmonary lobe.



**Central Picture.**

Intraoperative imaging detects a lung adenocarcinoma during a pulmonary resection.

**Table 1**

<b>n=50</b>	
Mean Age in Yrs (Range)	67 (25-85)
Gender	M = 27, F = 23
Mean Size in cm (Range)	2.6 (1.0-7.5)
Standardized uptake value (SUV)	5.1
Tumor Location	
	RUL 14
	RML 7
	RLL 10
	LUL 8
	LLL 11
Histologic Subtype	
	Acinar 24
	Papillary 9
	Solid 3
	Lepidic 7
	Mixed 7
Histologic Grade	
	Poor 18
	Moderate 23
	Well 6
Adenocarcinoma in situ/minimally invasive adenocarcinoma	3
In Situ tumor-to-background ratio	
	Fluorescent 1.7
	Non-Fluorescent 1.1
Tumor Exposed tumor to background ratio	
	Fluorescent 4.2
	Non-Fluorescent 0.9